SERI/TP-212-2323
UC Category: 63
DE84004508

$CdS/CuInSe_2$ Heterojunction Cell Research

R. Noufi
R. Axton
D. Cahen
S. K. Deb

May 1984

Presented at the IEEE 17th
Photovoltaics Specialists Conference
1-5 May 1984
Orlanda, Florida

Prepared under Task No. 3423.20
FTP No. 461

Solar Energy Research Institute
A Division of Midwest Research Institute

1617 Cole Boulevard
Golden, Colorado 80401

Prepared for the
U.S. Department of Energy
Contract No. DE-AC02-83CH10093

Printed in the United States of America
Available from:
National Technical Information Service
U.S. Department of Commerce
5285 Port Royal Road
Springfield, VA 22161
Price:
Microfiche A01
Printed Copy A02

$CdS/CuInSe_2$ HETEROJUNCTION CELL RESEARCH

R. Noufi, R. Axton, D. Cahen, and S. K. Deb
Solar Energy Research Institute
1617 Cole Blvd.
Golden, Colorado 80401

ABSTRACT

The objective of this research is (1) to fabricate and characterize $CuInSe_2$ thin films and (2) to fabricate and characterize $CdS/CuInSe_2$ solar cells. The material can be deposited either n- or p-type with mobilities of up to 150 cm^2/V s and carrier concentrations ranging from 10^{13}-10^{20} cm^{-3}. X-ray diffraction reveals a single phase with strong preferred orientation along <211> and <112> directions. The basic device structure of the cell consists of two $CuInSe_2$ layers, varying in the stoichiometry of elements and electrical properties, and two layers of CdS. Composition studies as well as electrical property measurements of the two layers were carried out to illustrate the role of the two layers of $CuInSe_2$. The methods used and results are discussed in detail and a conclusion is drawn as to whether the two layers in an actual device can be eliminated by using a single layer of intermediate composition and electrical properties.

INTRODUCTION

In the past few years, rapid progress has been achieved in thin-film compound semiconductor solar cells. The most promising have been thin-film cells of $CdS/CuInSe_2$ (1-6). The efficiencies of these cells have approached 11% (7), the highest for any thin-film solar cell. Despite this progress, much quantitative and qualitative information about the materials in these cells remained unknown. This lack of information presented a barrier to the understanding of the crucial properties and anomalous behaviors of these cells and caused some slowdown in progress.

SERI's effort in this regard has concentrated on three areas:

1. Material deposition and characterization
2. The role of the two $CuInSe_2$ layers necessary for high efficiency
3. Device fabrication and characterization.

The expected results of this effort are an improved understanding of the mechanisms controlling the growth of $CuInSe_2$ and CdS, and thorough knowledge of the chemistry and physics of these materials in order to optimize the resulting solar cell performance.

MATERIAL DEPOSITION AND CHARACTERIZATION

The vacuum evaporation system at SERI is a multisource system having the following sources: Cu, In, Se, CdS, and In for CdS doping. The usual deposition conditions needed to produce optimum results are shown in Table 1.

Table 1. Deposition Conditions for Producing Optimum Solar Cell Results

	Cu_1	In_1	Se_1	Cu_2	In_2	Se_2
Pressure (torr)		$3x10^{-6}$			$3x10^{-6}$	
Substrate temperature (°C)		350			450	
Deposition rate (Å/s)	3.6	3.0	15	2.9	3.0	15
Desired thickness (μm)		2.5			0.8	
Time (min)		~40			~17	

Subscripts 1 and 2 in Table 1 refer to the layers adjacent to the back contact and the heterojunction, respectively. Specifically, the system is brought up to the conditions of the first layer, at which time the substrate is exposed to evaporants. After the desired thickness of the first layer is achieved, the substrate temperature is brought up to 450°C from 350°C and the copper deposition rate is dropped to 2.9Å/s. This change in conditions takes about 5 seconds, while the substrate stays exposed to the evaporants. When the $CuInSe_2$ deposition is finished, the substrate is moved to the CdS compartment by remote control and the system is readied for CdS deposition. These conditions are given in a later section. Both n- and p-type films with carrier concentrations in the range of 10^{13}-10^{20} have been prepared. Hall mobilities in excess of 150 $cm^2/$ V s have been achieved. Most films are single-phase, with preferred orientation along the <211> and <112> directions.

The quality of the films was determined by characterizing their physical properties by several methods. The following are some characteristics of the films.

Optical Properties

The optical absorption edge is a function of stoichiometry, and it shifts to longer wavelength with increasing Cu/In ratio. Figures 1 through 3

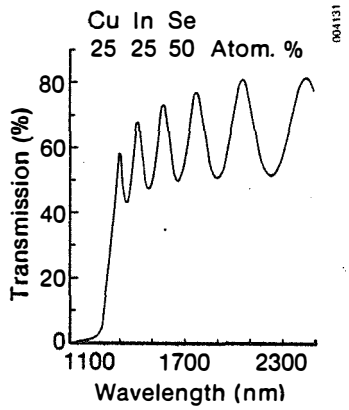

Figure 1. Transmission Spectrum of a $CuInSe_2$ Thin Film

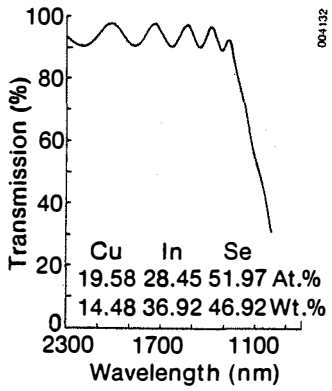

Figure 2. Transmission Spectrum of n-Type $CuInSe_2$ Thin Film

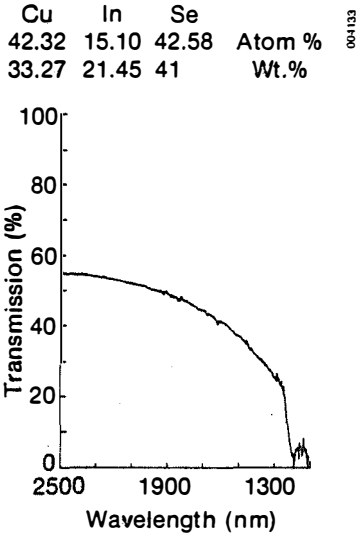

Figure 3. Transmission Spectrum of p-Type $CuInSe_2$ Thin Film

show the transmission spectrum for $CuInSe_2$ thin films of various compositions. Figure 1 is a typical spectrum of a near stoichiometric film with a composition as shown on the figure. This composition (hence, spectrum) is that of a $CuInSe_2$ thin-film layer adjacent to a back contact (Mo) in a finished CdS/ $CuInSe_2$ cell. Figure 2 shows the spectrum and corresponding composition of a $CuInSe_2$ layer adjacent to the heterojunction. Figure 3 shows the poor transmission characteristics of a very copper-rich film. This poor transmission is thought to be due to free carrier absorption and diffusivity of light at the longer wavelength end and defects of high disorder due to excess copper at the shorter wavelength end. The absorption coefficient for near stoichiometric films is greater than 10^5/cm.

Composition

The stoichiometry of the films was determined by electron microprobe analysis and by Auger spectroscopy. Figure 4 is an Auger depth profile of 2.5-μm-thick near-stoichiometric film, typical of the films composing the layer adjacent to the Mo back contact. The depth profile of a typical layer (0.8 μm) adjacent to the junction is shown in Figure 5. This layer is copper-poor. The depth profile and resulting composition of the two layers deposited on top of each are discussed in detail in a later section. Note, however, that the near-surface composition is usually richer in selenium than the bulk.

Morphology

The morphology of the $CuInSe_2$ films depends greatly on the composition, specifically on the Cu:In ratio. Films that are copper poor are silver/grey, shiny, and very smooth. Figure 6 shows a SEM picture of films typical of the layer adjacent to the junction. Note the lack of distinct features and grain definition. On the other hand, near-stoichiometric films are matte grey in color with distinct features and grains (Figure 7). Their grain size is relatively small. Films that are copper-rich (i.e., Cu/In ratio >> 1) are usually bluish in color and have distinct grains. Analysis of these films usually reveals a precipitate of $Cu_{2-x}Se$.

Stoichiometry vs. Electrical Properties

A series of films of different stoichiometry were prepared and their electrical properties probed. The electrical properties were obtained by means of several measurement techniques; i.e., Hall measurements, four probes, hot probe, and C-V.

In order to quantify the relationship between stoichiometry and electrical properties, a plot of carrier concentration vs. the Cu/In ratio is shown in Figure 8, which shows a narrow region of stoichiometry where p-$CuInSe_2$ of the desired carrier concentration and resistivity can be obtained. It is clear from the figure that in order to obtain p-$CuInSe_2$ films of the quality needed to produce a relatively high-efficiency CdS/$CuInSe_2$ solar cell,

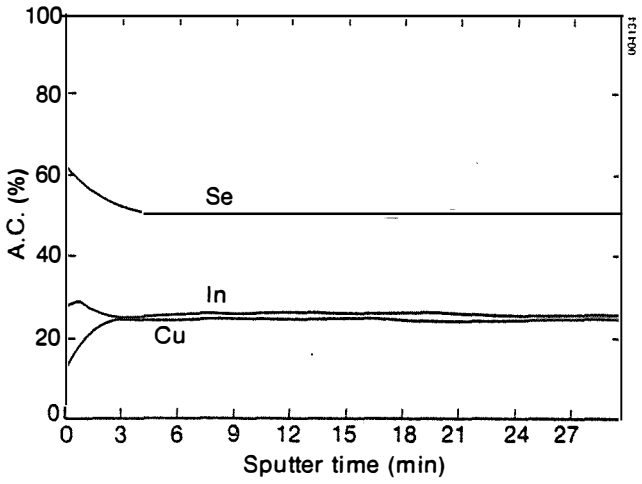

Figure 4. Auger Profile of a Near-Stoichiometric $CuInSe_2$ Thin Film

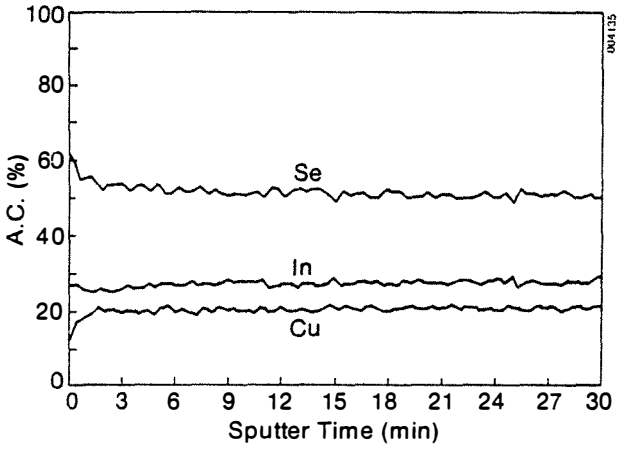

Figure 5. Auger Profile of a $CuInSe_2$ Thin Film

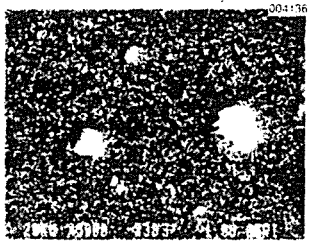

At %	
Cu	21
In	29
Se	50

Figure 6. SEM of a Copper-Poor $CuInSe_2$ Thin Film

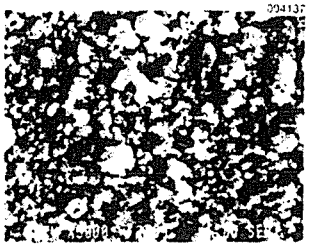

At %	
Cu	25
In	25
Se	50

Figure 7. SEM of a Stoichiometric $CuInSe_2$ Thin Film

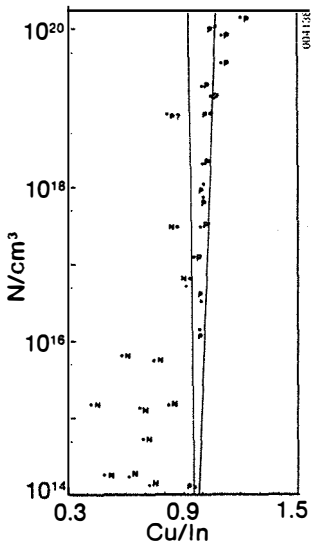

Figure 8. Stoichiometry vs. Carrier Concentration for $CuInSe_2$ Thin Film

one has to have very good control of the deposition conditions. The V-shaped region contains the chalcopyrite p-$CuInSe_2$, while in the region to the right of it, where it is copper-rich, the films reveal $CuInSe_2$ with a precipitate of $Cu_{2-x}Se$. The measured carrier concentration type is of p-character. In the region to the left, where copper is excessively poor, the films are n-type with a wide range of resistivity values. X-ray diffraction measurements also reveal various phases that are indium-rich.

The effect of the Se/metal (Cu + In) ratio on the carrier concentration of a p-type $CuInSe_2$ film within the v-shaped region is illustrated in Figure 9. It is interesting to note that in both cases the material is p-type when the sample is deficient in selenium. If we assume that the metals are occupying the regular lattice sites, then a Se deficiency should create anion vacancies that would act as donors. The p-type behavior could be accounted for if the excess indium exists in the reduced divalent and/or monovalent states, which results in the creation of acceptor states. For a fixed Se/M ratio (viz., Se/M = 0.95), the density of holes increases by almost two orders of magnitude when the Cu:In ratio is decreased from 0.98 to 0.96. This would imply that Cu-vacancy is primarily responsible for p-type conductivity. It is also instructive to note that as the material is made more nearly stoichiometric, the carrier concentration becomes more sensitive to the Se-deficiency.

In conclusion, we have shown here that the control of electrical properties of the $CuInSe_2$ film and, hence, the device efficiency, require an extremely tight control of stoichiometry. The electrical properties are dominated by native defects. Unravelling the defect structure is not a trivial problem and will require extensive theoretical and experimental studies. It is possible to make the following qualitative observation on the dependence of electrical properties on composition as derived from experimental data:

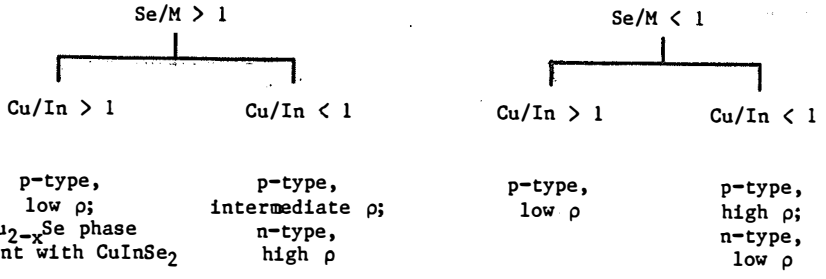

M = metal (Cu + In), ρ = resistivity.

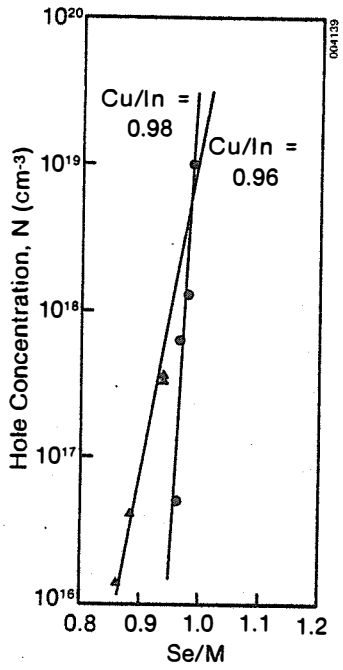

Figure 9. Hole Concentration vs. Se/M at Fixed Cu/In (M = metal)

THE ROLE OF HIGH- AND LOW-RESISTIVITY LAYERS

To study the role of the two $CuInSe_2$ layers, we prepared and analyzed two-layer films having varying compositions and partially overlapped structures for solid state properties. Each deposition resulted in a low- and high-resistivity film as well as an overlap region of the two (Figure 10).

Composition studies were carried out by electron microprobe which revealed that the overlap region had a composition intermediate between the two single layers. Table 2 summarizes some of the results. Note that we refer to the high-resistivity layer as n-type and the low-resistivity layer as p-type. This is because, most often, the layers prepared for the investigation had these distinctions. Auger depth profiling, as shown in Figure 11, of the overlap region shows a complete mix between the two layers. Layers prepared at a substrate temperature of only 350°C show less mixing (Figure 12), and we see distinctly from the Auger profile the boundary between the two compositions. These layers form a homojunction that exhibits up to 300 mV of photovoltage and up to 60 μA of short-circuit current. Hall measurements on these overlap layers also reveal electrical properties falling between those of the two individual regions. Table 3 summarizes these results. The morphology of the three regions, as shown in Figure 13, changes distinctively upon mixing; thus, grain sizes also change.

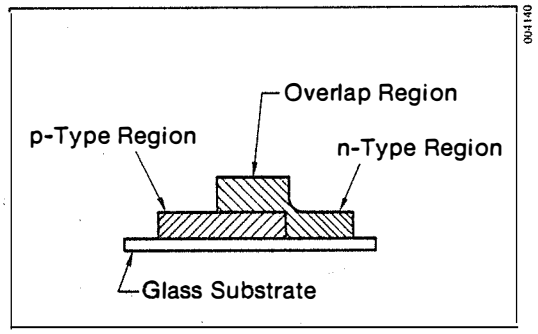

Figure 10. Schematic of a Two-Layer Overlap $CuInSe_2$ Thin Film

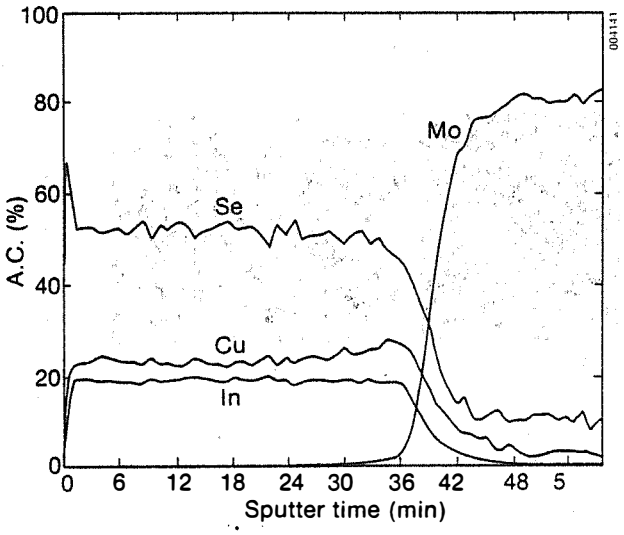

Figure 11. Auger Profile of a Two-Layer $CuInSe_2$ Thin Film

Table 2. Composition of the n-Type, p-Type and Overlap Regions

n-Type Region			
Sample	Wt. %		
	Cu	In	Se
1	13.4	38.8	47.8
2	14.0	38.0	48.0
3	14.7	37.5	47.7
4	15.4	37.1	47.5

p-type Region			
Sample	Wt. %		
	Cu	In	Se
1	30.1	25.9	44.0
2	30.6	25.7	43.6
3	34.5	22.2	43.2
4	35.3	21.9	42.8

Overlap Region			
Sample	Wt. %		
	Cu	In	Se
1	22.0	32.6	45.4
2	22.5	32.8	44.7
3	24.4	30.8	44.8
4	26.0	29.7	44.3

Table 3. Electrical Properties of the Three Regions

	n-type Region	Overlap Region	p-type Region
N/cm^3	2.3×10^{18}	3.9×10^{19}	9×10^{19}
ohm-cm	1×10^{-1}	4×10^{-2}	1.3×10^{-2}
$cm^2/V \cdot s$	3	4	5
N/cm^3	3.2×10^{13}	3.3×10^{15}	1.1×10^{16}
ohm-cm	5.7×10^{3}	2×10^{2}	1.6×10^{2}
$cm^2/V \cdot s$	34	10	4

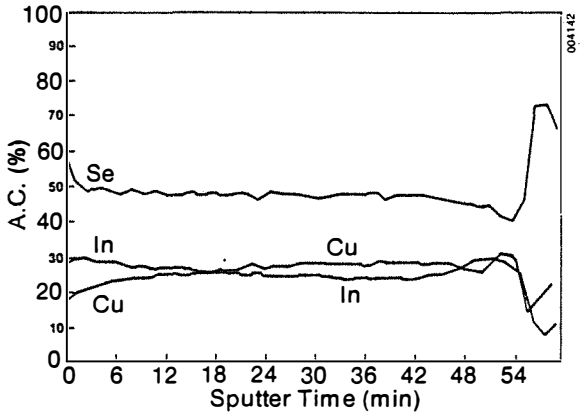

Figure 12. Auger Profile of a Two-Layer $CuInSe_2$ Thin Film

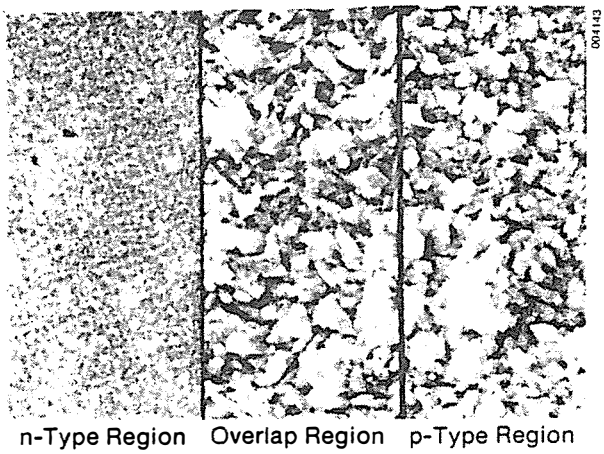

Figure 13. Morophology of the $CuInSe_2$ (Three Regions) Overlap Layer

Investigations continue on the role of the overlap layers. The conditions under which copper and indium diffuse will be studied systematically as a function of temperature and relative composition. Solar cells from these overlap layers will be constructed and their characteristics correlated. The purpose is to find out if a condition exists under which one intermediate layer of $CuInSe_2$ can be prepared and incorporated in an actual high-efficiency device, thus eliminating the need for the more complicated two $CuInSe_2$ layered cells.

DEVICE FABRICATION AND CHARACTERIZATION

CdS deposition takes place without breaking the vacuum in two stages: (1) deposition of undoped layers of about 0.8 μm after the deposition of $CuInSe_2$. This is a high-resistivity layer with values between 10^2 and 10^3 ohm-cm. (2) A second layer of CdS (2.5 μm) is deposited on top of the first layer. The resistivity of this layer is about 10^{-3} ohm-cm. The resultant resistivity of the two layers is between 10 and 0.3 ohm-cm. Both layers are deposited at a substrate temperature of 200°C and rate of 150 Å/s. The device is thus completed by the electron-beam evaporation of an Al grid pattern as a front contact. At this point in the device fabrication, the measured output characteristics are poor. Annealing of the device at 200°C in air for 20-30 minutes increases the output parameters greatly. The electron-beam-induced current (EBIC) of a cell before and after heat treatment is illustrated in Figures 14 and 15. Investigations are under way to understand the mechanisms of this last step in the fabrication.

The best device parameters obtained in this laboratory to date are as follows: open-circuit voltage (V_{oc}) = 0.395 V, short-circuit current density (J_{sc}) = 34.5 mA/cm^2, fill factor (FF) = 65.3%, and active area = 0.048 cm^2. The efficiency, based on active area is 8.9% (Figure 16).

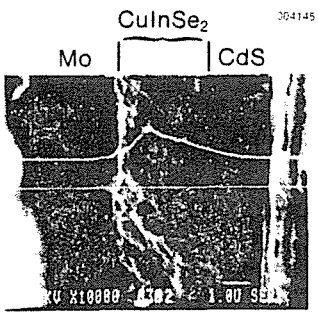

Figure 14. EBIC Scan of a Cds/$CuInSe_2$ Thin Film Solar Cell before Oxygen Bake

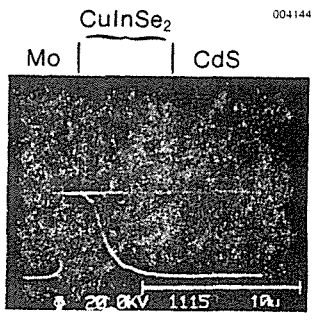

Figure 15. EBIC Scan of a Cds/$CuInSe_2$ Thin Film

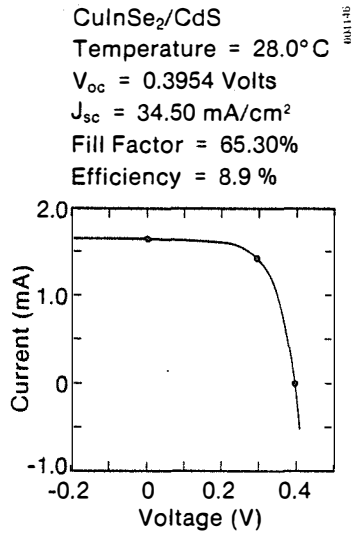

Figure 16. I-V Curve for All Thin Film $CuInSe_2$/CdS Solar Cell

ACKNOWLEDGMENT

The authors wish to acknowledge R. Ahrenkiel, R. Matson, C. Herrington, L. Kazmerski, and T. Coutts for their assistance with the measurements. This work is supported by the U.S. Department of Energy at the Solar Energy Research Institute under U.S. DOE Contract No. DE-AC02-83CH10093.

REFERENCES

1. J. L. Shay and J. H. Wernick, Ternary Chalcopyrite Semiconductors, Pergamon Press, New York, pp. 112, 175-214, 1975.

2. P. Yu, Y. S. Park, S. P. Faile, and J. E. Ehret, Appl. Phys. Lett.,26, 717, 1975.

3. S. M. Meese, J. C. Manthuruthil, and D. R. Locker, Bull. Am. Phys. Soc., 20, 696, 1975.

4. S. Wagner, J. L. Shay, P. Migliorato, and H. M. Kasper, Appl. Phys. Lett., 25, 434, 1974.

5. J. L. Shay, S. Wagner, K. Bachmann, E. Buehler, and H. M. Kasper, Proc. 11th IEEE Photovoltaics Spec. Conf., Phoenix, AZ, pp. 503-507, 1975.

6. W. S. Chen and R. A. Mickelsen, Proc. Soc. Photo. Opt. Instrum. Eng., 248, 62, 1981; R. A. Mickelsen and W. S. Chen, Proc. 15th IEEE PV Spec. Conf., Orlando, FL, IEEE, New York, pp. 800-804, 1981.

7. R. Hsiao, W. S. Chen, and R. A. Mickelsen, Abstracts: Polycrystalline Thin Film Review Meeting, The Solar Energy Research Institute, Golden, CO, p. 25, May 1983.